Available online at www.sciencedirect.com
SCIENCE DIRECT®
Journal of Sound and Vibration 285 (2005) 1151–1170
JOURNAL OF SOUND AND VIBRATION
www.elsevier.com/locate/jsvi

Dynamics and synchronization of coupled self-sustained electromechanical devices

R. Yamapi*, P. Woafo

Laboratoire de Mécanique, Faculté des Sciences, Université de Yaoundé I, B.P. 812, Yaoundé, Cameroon

Received 23 April 2003; accepted 20 September 2004
Available online 15 December 2004

Abstract

The dynamics and synchronization of two coupled self-excited devices are considered. The stability and duration of the synchronization process between two coupled self-sustained electrical oscillators described by the Rayleigh–Duffing oscillator are first analyzed. The properties of the Hill equation and the Whittaker method are used to derive the stability conditions of the synchronization process. Secondly, the averaging method is used to find the amplitudes of the oscillatory states of the self-sustained electromechanical device, consisting of an electrical Rayleigh–Duffing oscillator coupled magnetically to a linear mechanical oscillator. The synchronization of two such coupled devices is discussed and the stability boundaries of the synchronization process are derived using the Floquet theory and the Hill's determinant. Good agreement is obtained between the analytical and numerical results.

1. Introduction

The field of nonlinear science has seen a growing interest in the control and synchronization of nonlinear oscillators, both in their regular and chaotic states. The synchronization of chaotic oscillators was put on by Pecora and Carrol [1] by coupling both oscillators with a common drive signal. Latter on, Kapitaniak [2] showed that one can also synchronize two chaotic oscillators using the continuous feedback scheme developed by Pyragas [3]. The great interest devoted to

*Corresponding author. Tel.: +237 932 9376; fax: +237 222 6275.
E-mail addresses: ryamapi@yahoo.fr (R. Yamapi), pwoafo@uycdc.uninet.cm (P. Woafo).

0022-460X/$ - see front matter © 2004 Elsevier Ltd. All rights reserved.
doi:10.1016/j.jsv.2004.09.011

such topic is due to its potential applications in communications engineering (using chaos to mask the information-bearing signals) [1,4–6], in biology and chemistry [7,8].

The electromechanical engineering is another field where synchronization is of particular interest, e.g., for automation process, electromechanical devices should work in a synchronized manner with or without delay. This paper considers the dynamics and synchronization of self-sustained electromechanical devices consisting of an electrical Rayleigh–Duffing oscillator coupled magnetically to a linear mechanical oscillator. The study uses the continuous feedback scheme of Pyragas [3]. The Whittaker method [9] and the Floquet theory [9,10] are used to derive the stability boundaries and the optimal coupling strength for the synchronization process.

Two main points are considered. In Section 2, the problem of synchronizing two coupled self-sustained electrical oscillators described by the Rayleigh–Duffing oscillator is first analyzed. After the presentation of the model and statement of the problem, the analytic study of the stability of the synchronization process and the derivation of the expressions for the synchronization time are carried out. The analytical results are then compared to the numerical ones. The second point is the study of the dynamics and synchronization of self-sustained electromechanical devices. For this aim, the amplitudes of the oscillatory states are obtained using the averaging method [9,10]. The synchronization of two coupled self-sustained electromechanical devices is then discussed. The stability boundaries of the synchronization process are derived using the Floquet theory [9,10]. Conclusion is given in the last section.

2. The self-sustained electrical model

2.1. The model and statement of the problem

The model shown in Fig. 1 is a self-excited electrical system described by the Rayleigh–Duffing oscillator, consisting of a nonlinear resistor NLR, a condenser C and an inductor L, all connected in series. Two types of nonlinear components are considered in the model. The voltage of the condenser is a nonlinear function of the instantaneous electrical charge q is expressed by

$$V_C = \frac{1}{C_0} q + a_3 q^3, \tag{1}$$

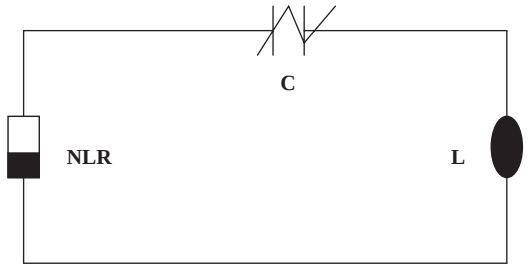

Fig. 1. Schematic of a self-sustained electrical model.

where C_0 is the linear value of C and a_3 is a nonlinear coefficient depending on the type of the capacitor in use. This is typical of nonlinear reactance components such as varactor diodes widely used in many areas of electrical engineering to design for instance parametric amplifiers, up-converters, mixers, low-power microwave oscillators, etc. [13]. The current–voltage characteristic of a resistor is also defined as

$$V_{R_0} = R_0 i_0 \left[-\left(\frac{i}{i_0}\right) + \left(\frac{i}{i_0}\right)^3 \right], \tag{2}$$

where R_0 and i_0 are, respectively, the normalization resistance and current. i is the value of current corresponding to the limit resistor voltage. In this case, the model has the property to exhibit self-excited oscillations. This is due to the presence of a nonlinear resistor whose current–voltage characteristic curve shows a negative slope, and the fact that the model incorporates through its nonlinear resistance a dissipative mechanism to damp oscillations that grow too large and a source of energy to pump up those that become small. Because of this particular behavior, we can qualify our model as a self-sustained electrical model. This nonlinear resistor can be realized using a block consisting of two transistors [14].

Using the electrical laws, it is found that the model is described by the following differential equation:

$$L\frac{\mathrm{d}^2 q}{\mathrm{d}\tau^2} - R_0\left[1 - \frac{1}{i_0^2}\left(\frac{\mathrm{d}q}{\mathrm{d}\tau}\right)^2\right]\frac{\mathrm{d}q}{\mathrm{d}\tau} + \frac{q}{C_0} + a_3 q^3 = 0. \tag{3}$$

The substitution of the quantities

$$w_e^2 = \frac{1}{LC_0}, \quad t = w_e\tau, \quad \alpha_0 = \frac{q_0^2 w_e^2}{i_0^2}, \quad x = \frac{q}{q_0}, \quad \mu = \frac{R_0}{Lw_e}, \quad \alpha = \frac{a_3 q_0^2}{Lw_e^2}$$

yields the following Rayleigh–Duffing equation:

$$\ddot{x} - \mu(1 - \alpha_0\dot{x}^2)\dot{x} + x + \alpha x^3 = 0, \tag{4}$$

where q_0 is the reference charge of q, the dots over the quantities represent the derivative with respect to time t, μ, α_0 and α are three positive coefficients. Eq. (4) is the Rayleigh–Duffing equation, which has many applications in science and engineering, particularly when the model shown in Fig. 1 is connected mutually, such as a ring of mutually coupled self-sustained electrical systems. For mathematical convenience, we set $\alpha_0 = 1$ in the rest of the paper. It is important to note that the Rayleigh–Duffing oscillator has a similar behavior such as the Van der Pol–Duffing oscillator, so that it displays a rich variety of nonlinear dynamical behaviors [11,12]. It generates the limit cycle, which can (for a low value of the coefficient μ) be approximated by the harmonic function of time defined as

$$x(t) = a\cos(w_0 t - \phi_0), \tag{5}$$

where $a = \frac{2}{3}\sqrt{3}$, ϕ_0 the phase and the limit cycle frequency corresponding to $w_0^2 = 1 + \frac{3}{8}\alpha a^2$. This limit cycle is known to be a fairly strong attractor since it attracts all trajectories except the one initiated from the trivial fixed point $(x_0, \dot{x}_0) = (0, 0)$. As the Van der Pol oscillator, a particular

characteristic in the Rayleigh–Duffing model is that its phase depends on initial conditions. Consequently, if two Rayleigh–Duffing oscillators are launched with different initial conditions, their trajectory will finally circulate on the same limit cycle, but with different phases ϕ_1 and ϕ_2. The objective of the synchronization in this case is to phase-lock so that $\phi_1 - \phi_2 = 0$.

In view of studying the phase-locking or synchronization of nonlinear oscillators, Leung in Ref. [15] considered the synchronization of two self-excited oscillators with various types of couplings, including the continuous feedback difference coupling of Pyragas [3]. In particular, he showed that synchronization is possible for some appropriate ranges of the coupling strength and that the synchronization time has a critical slowing-down character near the boundaries of the synchronization domain. Recently, Woafo and Kraenkel [16] considered the problem of stability and duration of the synchronization process between classical Van der Pol oscillators and showed that the critical slowing-down behavior of the synchronization time and the boundaries of the synchronization domain can be estimated by analytical investigations. The next sub-section of this paper extends the calculations of Ref. [16] to two coupled Rayleigh–Duffing oscillators. The master system is described by the component x, while the slave system has the corresponding component u. The enslavement is carried out by coupling the slave to the master through the following scheme:

$$\begin{aligned} &\ddot{x} - \mu(1 - \dot{x}^2)\dot{x} + x + \alpha x^3 = 0, \\ &\ddot{u} - \mu(1 - \dot{u}^2)\dot{u} + u + \alpha u^3 = -K(u - x)H(t - T_0), \end{aligned} \tag{6}$$

where K is the feedback coupling coefficient, t the time, T_0 is the onset time of the synchronization process and $H(x_1)$ is the Heaviside function defined as

$$H(x_1) = \begin{cases} 0 & \text{for } x_1 < 0, \\ 1 & \text{for } x_1 \geqslant 0. \end{cases}$$

The schematic circuit of two coupled identical self-sustained electrical models with a unidirectionally homogenous coupling element is shown in Fig. 2. In this circuit, the two self-sustained models, namely, the master and slave, are coupled by a linear resistor R_c and a buffer. The buffer acts a signal-driving element that isolates the master system variable from the slave system variable, thereby providing a one-way coupling or unidirectional coupling. In the absence of the buffer, the system represents two identical self-sustained models coupled by a common resistor R_c, when both the master and slave systems will mutually affect each other.

2.2. Synchronization of two self-sustained electrical models

When the synchronization process is launched, the slave system changes its configuration and it is of interest to determine the range of K for the synchronization process to be achieved or stable. Indeed, the model is physically interesting only if the dynamics of the slave is stable. Let us introduce the new variable

$$\varepsilon(t) = u(t) - x(t), \tag{7}$$

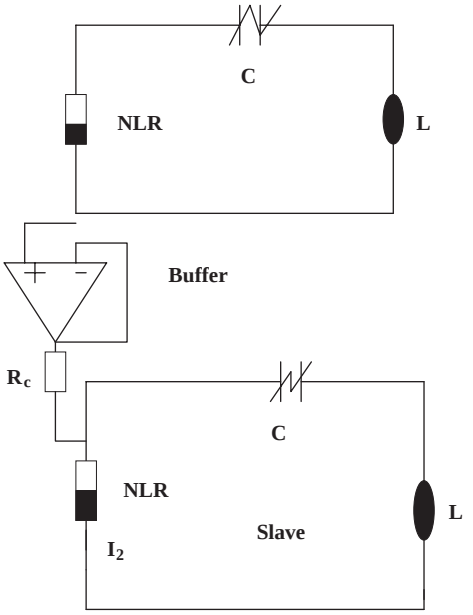

Fig. 2. Schematic of unidirectional coupled self-sustained electrical models.

which is the measure of the nearness of the slave to the master. ε obeys the linear variational equation

$$\ddot{\varepsilon} - \mu(1 - 3\dot{x}^2)\dot{\varepsilon} + (3\alpha x^2 + 1 + K)\varepsilon = 0. \tag{8}$$

Synchronization occurs when $\varepsilon(t)$ tends to zero as t increases, or is less than a given precision. The behavior of $\varepsilon(t)$ depends on K and on the form of the master x. For small value of μ, the master time evolution is described by Eq. (5). Thus, the linear variational equation (8) takes the form

$$\ddot{\varepsilon} + (2\lambda + F(\tau))\dot{\varepsilon} + G(\tau)\varepsilon = 0, \tag{9}$$

where

$$\tau = w_0 t - \phi_0, \quad \lambda = \frac{\mu}{2w_0}\left(\tfrac{3}{2}w_0^2 a^2 - 1\right), \quad F(\tau) = \frac{-3}{2}\, w_0 \mu a^2 \cos 2\tau,$$
$$G(\tau) = \frac{2K + 2 + 3\alpha a^2 + 3\alpha a^2 \cos 2\tau}{2w_0^2}.$$

From the expression of $G(\tau)$, we find that if

$$K < -\tfrac{3}{2}\alpha a^2 - 1, \tag{10}$$

$\varepsilon(t)$ will grow indefinitely, leading the slave to continuously drift away from its original limit cycle. In this case, the feedback coupling is dangerous since it continuously adds energy to the slave system. To examine the stability process, we first transform Eq. (9) into the standard form by

introducing a new variable η as follows:

$$\varepsilon = \eta \exp(-\lambda\tau)\exp\left\{-\frac{1}{2}\int_0^\tau F(\tau')\,\mathrm{d}\tau'\right\},$$
$$= \eta \exp\{-\lambda\tau + \tfrac{3}{8}w_0\mu a^2 \sin 2\tau\}. \tag{11}$$

This yields the following Hill equation:

$$\ddot{\eta} + (a_0 + 2a_{1s}\sin 2\tau + 2a_{1c}\cos 2\tau + 2a_{2c}\cos 4\tau)\eta = 0, \tag{12}$$

with

$$a_0 = \frac{2K + 2 + 3\alpha a^2}{2w_0^2} - \lambda^2 - \tfrac{9}{32}w_0^2\mu^2a^4,$$
$$a_{1s} = \tfrac{-3}{4}w_0\mu a^2, \quad a_{2c} = \tfrac{-9}{64}w_0^2\mu^2a^4,$$
$$a_{1c} = \tfrac{3}{4}\frac{\alpha a^2}{w_0^2} + \tfrac{3}{4}\mu\lambda w_0 a^2.$$

Following the Floquet theory [9,10], the solution of Eq. (9) may be either stable or unstable. The stability boundaries are found around the two main parametric resonances defined at $a_0 = n^2$ (with $n = 1, 2$). The solution of Eq. (12) in the nth unstable region may be assumed in the following form [9]:

$$\eta = \exp(\mu_0\tau)\sin(n\tau - \sigma), \tag{13}$$

where μ_0 is the characteristic exponent and σ a constant. Substituting Eq. (13) into Eq. (12) and equating the coefficients of $\cos n\tau$ and $\sin n\tau$ separately to zero, we obtain the following expression for the characteristic exponent:

$$\mu_0^2 = -(a_0 + n^2) + \sqrt{4n^2a_0 + a_n^2}, \tag{14}$$

with $a_n^2 = a_{nc}^2 + a_{ns}^2$.

Since the synchronization process is achieved when ε goes to zero with increasing time, the real parts of $-\lambda \pm \mu_0$ should be negative. Consequently, the synchronization process is stable under the condition

$$H_n = (a_0 - n^2)^2 + 2\lambda^2(a_0 + n^2) + \lambda^4 - a_n^2 > 0, \quad n = 1, 2. \tag{15}$$

In the second main parametric resonance (i.e. $n = 2$), condition (15) is satisfied ($H_2 > 0$). Then the stability is analyzed only in the first parametric resonance (i.e. $n = 1$).

We have checked for the validity of these criteria by solving numerically Eq. (6) for $\mu = 0.1, \alpha = 0.01$ and $\mu = 0.1, \alpha = 0.1$. The values of the amplitude a and the frequency w_0 are given before through analytical investigations (see Eq. (5)). In the case $\alpha = 0.01$, the analytical consideration gives that the synchronization process is stable for $K \in]-1.023; -0.107] \cup [0.09; +\infty[$, while numerically we find that the synchronization process is achieved if $K \in]-1.01; -0.06] \cup]0.03; +\infty[$. Here, the synchronization process is unstable, which means that $\varepsilon(t)$ never goes to zero, but may have a bounded oscillatory behavior. To illustrate this result, let us present graphically the time history of the deviation $\varepsilon(t)$ between the master and the slave

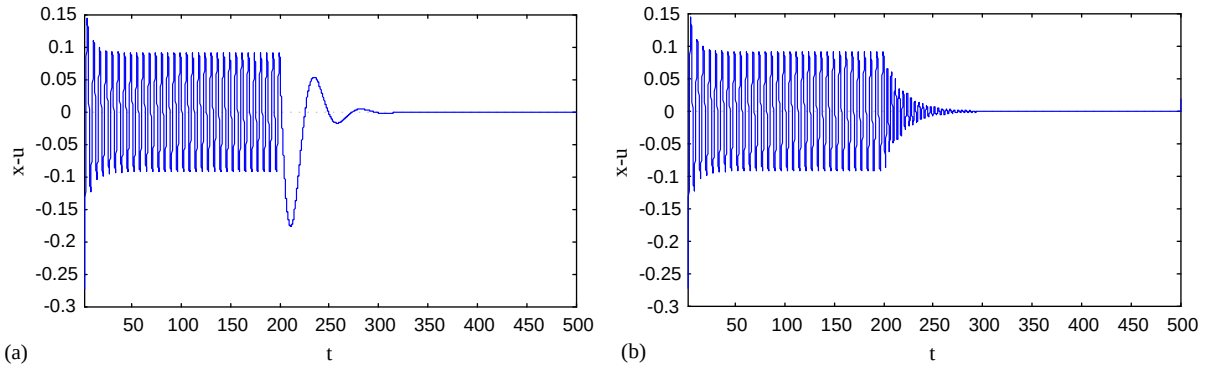

Fig. 3. Time history of the deviation $\varepsilon(t)$ for $\alpha = 0.01$, $\mu = 0.1$ with the value of the coupling coefficient K chosen in the stability domain. (a) $K = -1.0$, (b) $K = 1.5$.

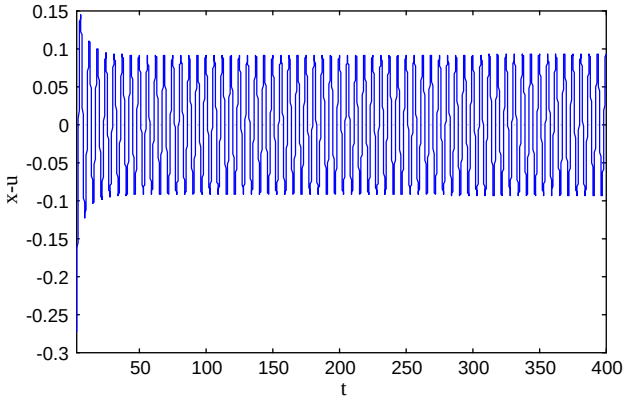

Fig. 4. Time history of the deviation $\varepsilon(t)$ for $\alpha = 0.01$, $\mu = 0.1$ with the value of the coupling coefficient K chosen in the instability domain. $K = -0.02$.

systems for a coupling coefficient K chosen both in the stable and unstable regions. In the stable domain, we find in Fig. 3 that the deviation $\varepsilon(t)$ goes to zero when the time goes up, while for the unstable region, the deviation $\varepsilon(t)$ has a bounded oscillatory behavior as it appears in Fig. 4. For the case $\alpha = 0.1$, it is found from our analytical consideration that the synchronization process is stable for $K \in]-1.203; -0.3] \cup]0.0; +\infty[$, while for the numerical simulation the synchronization process is achieved for the region of K defined as $K \in]-1.19; -0.2[\cup [0.006; +\infty[$. In both cases $\alpha = 0.01$ and 0.1, there is a fairly good agreement between the analytical and numerical results.

Let us now look for the synchronization time. It is defined as

$$T_s = t_s - T_0, \quad \forall t_s > T_0, \tag{16}$$

computed following the time trajectory of the slave system relative to that of the master, t_s is the time instant at which the two trajectories are close enough to be considered as synchronized.

Synchronization is achieved when $\varepsilon(t)$ obeys the following synchronization condition:

$$|\varepsilon(t)| = |u - x| < h, \quad \forall t > T_0, \tag{17}$$

where h is the synchronization precision or tolerance.

Near the resonant states, the solution $\varepsilon(t)$ of the variational equation (9) takes the form

$$\begin{aligned}\varepsilon(t) = \{&c_1 \exp[-(\lambda - \mu_0)(\tau - T_0)] \sin(n\tau - \sigma_1) \\ &+ c_2 \exp[-(-\lambda - \mu_0)(\tau - T_0)] \sin(n\tau - \sigma_2)\} \\ &\times \exp\left\{-\frac{1}{2}\int F(\tau')\,\mathrm{d}\tau'\right\},\end{aligned} \tag{18}$$

where c_1 and c_2 are two constants depending on initial conditions for $\varepsilon(t)$. The term proportional to c_2 decreases more quickly to zero. With the first term, we obtain the following expression for c_1:

$$c_1^2 = \varepsilon_s^2 + \left\{\frac{\dot{\varepsilon}_s + (\lambda - \mu_0)\varepsilon_s}{n^2}\right\}^2,$$

where ε_s and $\dot{\varepsilon}_s$ are the values of the deviation and its velocity at the time t_s. Thus, near the resonance states, the analytical expression of the synchronization time is obtained as

$$T_s = \frac{1}{\lambda - \mu_0} \ln \frac{c_1}{h}. \tag{19}$$

Far from the resonant states, the variational equation reduces to

$$\ddot{\varepsilon} + 2\lambda\dot{\varepsilon} + \Omega_1^2\varepsilon = 0, \tag{20}$$

with

$$\Omega_1^2 = \frac{2K + 2 + 3\alpha a^2}{2w_0^2}.$$

Following the procedure used above, the synchronization time depends on the sign of $\Delta = \Omega_1^2 - \lambda^2$ as follows:

- for $\Delta > 0$, we have

$$T_s = \frac{1}{\lambda} \ln \frac{b_0}{h}, \tag{21}$$

  with $b_0^2 = \varepsilon_s^2 + (\dot{\varepsilon}_s + \lambda\varepsilon_s)^2/\Delta$.
- for $\Delta < 0$, we have

$$T_s = \frac{1}{\sqrt{-\Delta} - \lambda} \ln \frac{c_0}{h}, \tag{22}$$

  with $c_0 = (\dot{\varepsilon}_s + \varepsilon_s[-\lambda + \sqrt{-\Delta}])/2(\sqrt{-\Delta} - \lambda)$.

The analytical results obtained from Eqs. (19), (21) and (22) are verified by a direct numerical simulation of Eq. (6) with the sixth-order formulas of the Butcher family of the Runge–Kutta algorithm [17]. The master and the slave are initially launched with the initial conditions $(x(0), \dot{x}(0)) = (4.0; 4.0)$ and $(u(0), \dot{u}(0)) = (5.0; 5.0)$, respectively. We use the precision $h = 10^{-10}$ to compute the synchronization time. The results are reported in Fig. 5, where the synchronization

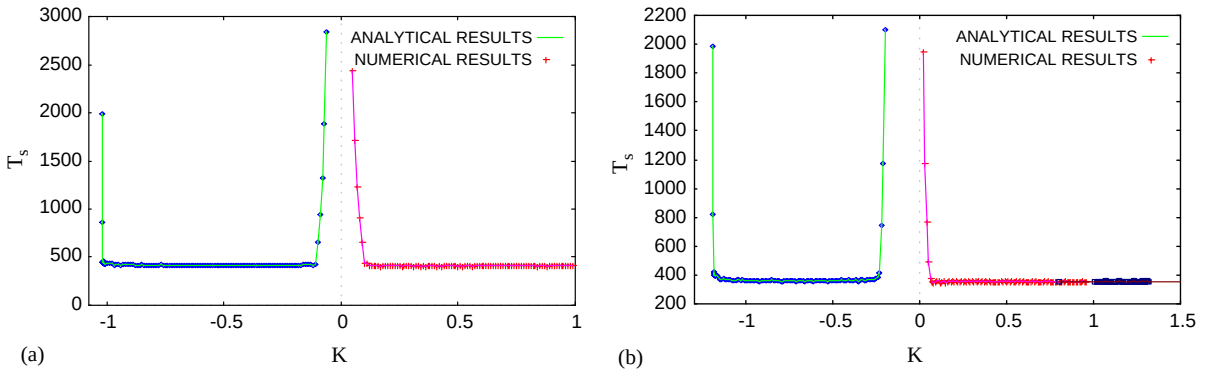

Fig. 5. Synchronization time versus the coupling coefficient K with the parameters $\mu = 0.1$; $T_0 = 200$ and the precision $h = 10^{-10}$, (—) for analytical results and (.+.) for numerical results, (a) $\alpha = 0.01$ and (b) $\alpha = 0.1$.

time is plotted versus the coupling coefficient K. The agreement between the analytical and the numerical results is good over the entire synchronization domains.

3. The self-sustained electromechanical device

3.1. Model and equations of motion

Section 2 has dealt with the synchronization of two self-excited oscillators of the Rayleigh–Duffing types. This self-excited oscillator can be associated to mechanical device to form a self-excited electromechanical device, which could be of practical interest in the automation engineering. Thus, the synchronized dynamics of two such devices is interesting and constitutes the topic of this Section 3. Shown in Fig. 6, the electromechanical device is composed of an electrical part coupled magnetically to a mechanical part. The coupling is realized through the electromagnetic force due to a permanent magnet. It creates a Laplace force in the mechanical part and the Lenz electromotive voltage in the electrical part. The electrical part is that presented in Subsection 2.1, while the mechanical part is composed of a mobile beam which can move along the $\vec{z}$-axis on both sides. Rod T, which has a similar motion, is bound to a mobile beam with a spring.

Using the electrical and mechanical laws, and taking into account the contributions of the Laplace force and the Lenz electromotive voltage, the electromechanical device is described by the following set of two coupled differential equations:

$$L\frac{d^2q}{d\tau^2} - R_0\left[1 - \frac{1}{i_0^2}\left(\frac{dq}{d\tau}\right)^2\right]\frac{dq}{d\tau} + \frac{q}{C_0} + a_3q^3 + lB_m\frac{dz}{d\tau} = 0,$$
$$m\frac{d^2z}{d\tau^2} + \lambda\frac{dz}{d\tau} + kz - lB_m\frac{dq}{d\tau} = 0, \tag{23}$$

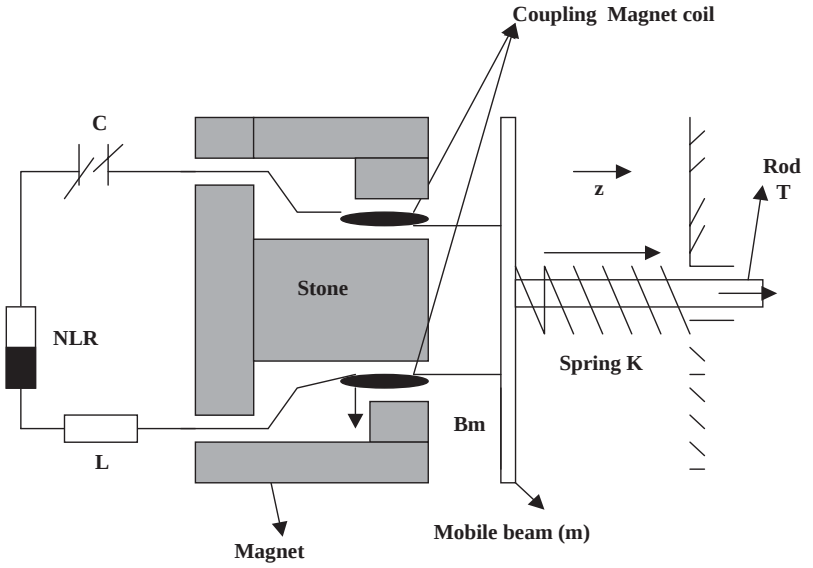

Fig. 6. Self-sustained electromechanical device.

where l is the length of the current wire in the domain of interaction between $\vec{B}_m$ and the two mobile rods supporting the beam. Let us use the dimensionless variables

$$x = \frac{q}{q_0}, \quad y = \frac{z}{l}, \quad t = w_e\tau$$

and

$$\beta = \frac{a_3 q_0^2}{L w_e^2}, \quad w_e^2 = \frac{1}{LC_0}, \quad w_m^2 = \frac{k}{m}, \quad w_2 = \frac{w_m}{w_e},$$
$$\mu_1 = \frac{R}{L w_e}, \quad \lambda_1 = \frac{l^2 B_m}{L q_0 w_e}, \quad \lambda_2 = \frac{B_m q_0}{m w_e}, \quad \gamma = \frac{\lambda}{m w_e}.$$

Then, the electromechanical device is described by the following set of two coupled nondimensional differential equations (we remind that $\alpha_0 = 1$):

$$\ddot{x} - \mu_1(1 - \dot{x}^2)\dot{x} + x + \beta x^3 + \lambda_1 \dot{y} = 0,$$
$$\ddot{y} + \gamma\dot{y} + w_2^2 y - \lambda_2 \dot{x} = 0, \tag{24}$$

where x and y are, respectively, the dimensionless electric charge in the condenser and the displacement of the mobile beam. μ_1 is a positive coefficient, γ the damping coefficient, w_2 the natural frequency, β the nonlinearity coefficient, λ_1 and λ_2 are the damping coupling coefficients. Thus, the equations of motion consist of the Rayleigh–Duffing oscillator coupled to the linear mechanical oscillator. With the presence of the Rayleigh–Duffing oscillator, the electromechanical transducer has the property to exhibit self-excited oscillations.

The model represented by Fig. 6 is widely encountered in various branches of electromechanical engineering. In particular, in its linear version, it describes the well-known electrodynamic loudspeaker [18]. In the self-excited nonlinear version, it can serve various applications such as autonomous devices in the cutting and drilling processes. Here one would like to take advantage of nonlinear responses of the model in manufacturing processes.

3.2. The resonant oscillatory states and quenching phenomena

Following the averaging method [9,10], the amplitudes A and B of x and y, and the phase difference ϕ between x and y satisfy the following set of first-order differential equations:

$$\begin{aligned}
\dot{A} &= -\tfrac{1}{2}\mu_1 A\left(1-\tfrac{3}{4}A^2\right)+\tfrac{1}{2}\lambda_1 w_2 B\cos\phi,\\
\dot{B} &= -\tfrac{1}{2}\gamma B+\frac{\lambda_2}{2w_2}A\cos\phi,\\
\dot{\phi} &= -\tfrac{3}{8}\beta A^2+\left\{\frac{\lambda_2 A}{2w_2 B}-\frac{\lambda_1 w_2 B}{2A}\right\}\sin\phi.
\end{aligned} \tag{25}$$

In the stationary state, A and B satisfy the following nonlinear algebraic equations

$$\begin{aligned}
&b_6A^6+b_4A^4+b_2A^2+b_0=0,\\
&B^2=MA^2(4-3A^2),
\end{aligned} \tag{26}$$

with the coefficients b_i and M defined as follows:

$$M=\frac{\mu_1\lambda_2}{4\gamma\lambda_1 w_2^2},$$

$$b_6=-\tfrac{27}{16}M\lambda_2^2w_2^2\beta^2-27M^3\lambda_1^2\gamma^2w_2^6,$$

$$b_4=\tfrac{9}{4}M\lambda_2^2w_2^2\beta^2-9M^2\lambda_2^2w_2^4\lambda_1^2-18M^2\lambda_1\lambda_2w_2^4\gamma^2+81M^3\gamma^2\lambda_1^2w_2^6,$$

$$b_2=24M^2\lambda_2^2\lambda_1^2w_2^4+16M^2\lambda_2\lambda_1\gamma^2w_2^4-3\gamma^2w_2^2M\lambda_2^2-6M\lambda_2^3\lambda_1w_2^2+48M^3\lambda_1^2\gamma^2w_2^6,$$

$$\begin{aligned}
b_0=&\,4M\lambda_2^2\gamma^2w_2^2+8M\lambda_2^3\lambda_1w_2^2-16M^2\lambda_2^2\lambda_1^2w_2^4\\
&+64M^3\lambda_1^2\gamma^2w_2^6-\lambda_2^4.
\end{aligned}$$

The equation in A can be solved using MATHEMATICA or the Newton–Raphson algorithm with the set of parameters: $\lambda_2=0.4,\ w_2=1.0,\ \mu_1=0.1,\ \beta=0.5$ and $\lambda_1=0.08$. Fig. 7 shows the response curves when the damping coefficient γ is varied. In the region $\gamma\in]0.12;0.304[$, a complete quenching phenomena of oscillations occurs. This region can also be obtained from the equation $b_0=0$, since $A=B=0$, and the quenching phenomena of oscillations occurs for γ satisfying the following equation:

$$\mu_1\lambda_2^3\gamma^3-\lambda_2^4\lambda_1\gamma^2+(2\mu_1\lambda_2^4\lambda_1+\mu_1^3\lambda_2^3)\gamma-\mu_1^2\lambda_2^4\lambda_1=0.$$

In this state, our model can serve as an electromechanical vibration absorber [19] of undesirable self-excited vibrations in mechanical systems. The quenching of self-excited oscillations had also

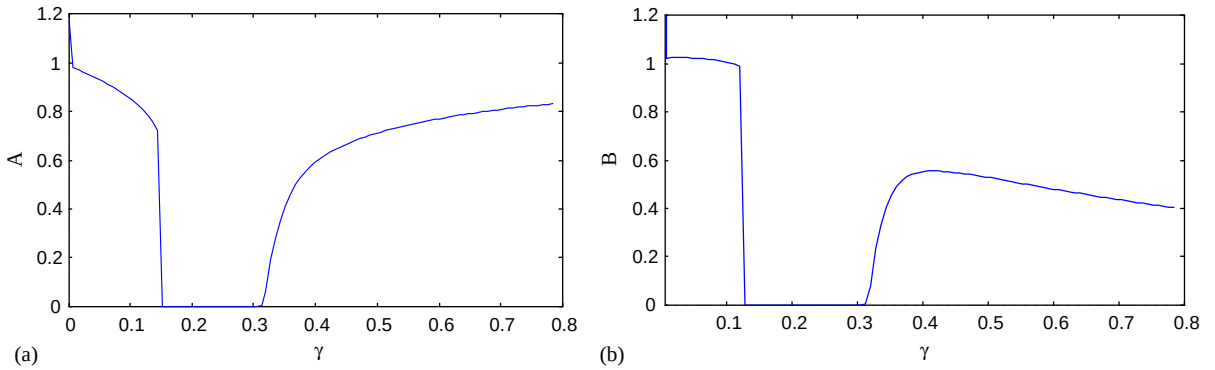

Fig. 7. The steady states A (a) and B (b) versus the damping coefficient γ for $\mu_1 = 0.1$; $\beta = 0.5$; $\lambda_1 = 0.08$; $\lambda_2 = 0.4$; $w_2 = 1.0$.

been reported in Refs. [20,21], for the Van der Pol oscillator coupled to a linear oscillator using Lanchester damper. But here, the quenching of mechanical self-excited oscillations could be insured by an appropriate choice of the components of an electrical circuit (assuming that the mechanical oscillator is described by the nonlinear oscillator and the electrical circuit by the linear oscillator).

3.3. Synchronization of two self-sustained electromechanical devices

As we have seen in the previous section, due to the presence of the self-excited oscillator in the model, the final state of the electromechanical device is a sinusoidal limit cycle and its phases ϕ_k depend on initial conditions. Consequently, if two self-sustained electromechanical devices are launched with different initial conditions, their trajectory will finally circulate on the same limit cycle, but with different phases ϕ_k. We derive now the characteristics of the synchronization of two self-sustained electromechanical devices. The master system is described by the components x and y, while the slave system has the corresponding components u and v. The enslavement is carried out by coupling the slave to the master through the following scheme:

$$\begin{aligned}
&\ddot{x} - \mu_1(1 - \dot{x}^2)\dot{x} + x + \beta x^3 + \lambda_1 \dot{y} = 0,\\
&\ddot{y} + \gamma\dot{y} + w_2^2 y - \lambda_2 \dot{x} = 0,\\
&\ddot{u} - \mu_1(1 - \dot{u}^2)\dot{u} + u + \beta u^3 + \lambda_1 \dot{v} = -K(u - x)H(t - T_0),\\
&\ddot{v} + \gamma\dot{v} + w_2^2 v - \lambda_2 \dot{u} = 0.
\end{aligned} \tag{27}$$

Practically, this type of unidirectional coupling between the master system and the slave system can be done as it is shown in Fig. 8. The two self-sustained electromechanical devices are coupled by a linear resistor R_c and a buffer. We remind that the buffer acts a signal-driving element that isolates the master system variables from the slave system variables, thereby providing a one-way coupling. In the absence of the buffer, the system represents two identical self-sustained

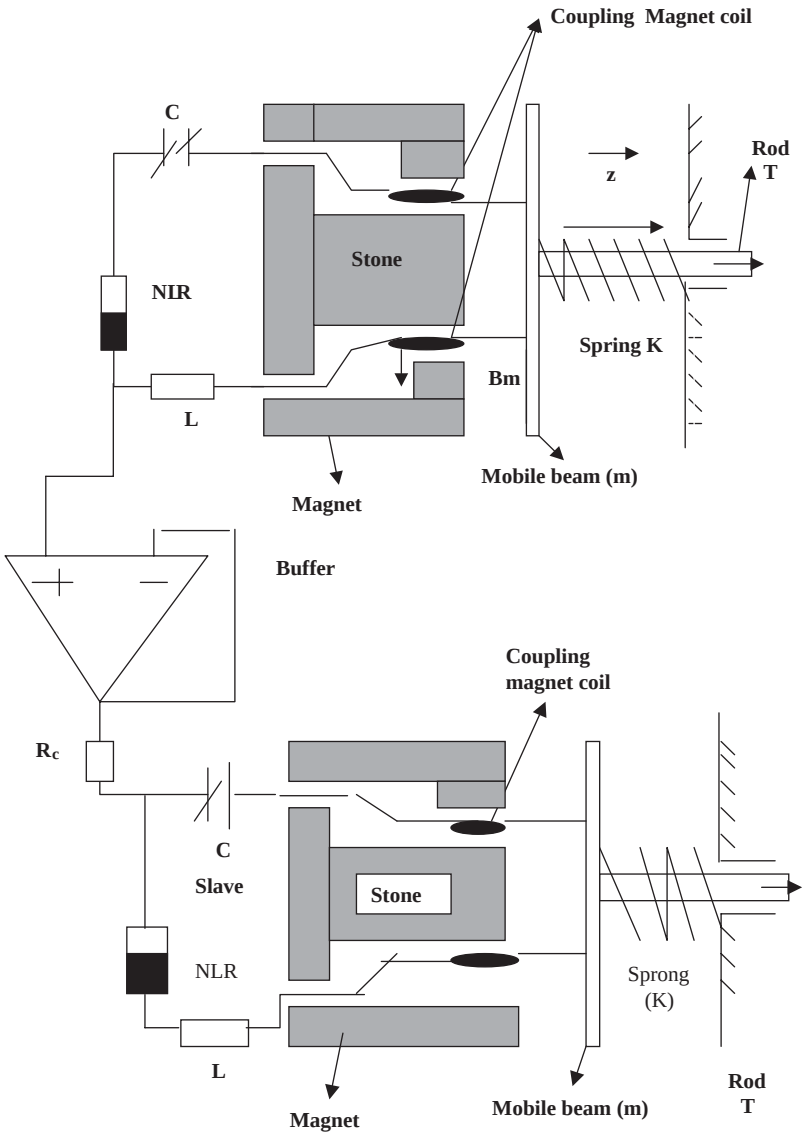

Fig. 8. Schematic of unidirectionally coupled self-sustained electromechanical devices.

electromechanical devices coupled by a common resistor R_c, when both the master and slave systems will mutually affect each other.

As we note before, the synchronization process is physically interesting only if the dynamics of the slave is stable and follows that of the master. Let us introduce the variables

$$\varepsilon_1(t) = u(t) - x(t),$$
$$\varepsilon_2(t) = v(t) - y(t). \tag{28}$$

To examine the stability of the synchronization process, let us look for the conditions of boundedness of ε_i which in the linear regime obey the following equations:

$$\begin{aligned}&\ddot{\varepsilon}_1 - \mu_1(1 - 3\dot{x}^2)\dot{\varepsilon}_1 + [1 + K + 3\beta x^2]\varepsilon_1 + \lambda_1\dot{\varepsilon}_2 = 0,\\&\ddot{\varepsilon}_2 + w_2^2\varepsilon_2 + \gamma\dot{\varepsilon}_2 - \lambda_2\dot{\varepsilon}_1 = 0.\end{aligned} \tag{29}$$

The behavior of ε_i depends on K and on the form of the master (x, y). The master time evolution can be described by

$$\begin{aligned}x &= A\cos(wt - \phi_1),\\y &= B\cos(wt - \phi_2),\end{aligned} \tag{30}$$

where the amplitudes A and B, and the phases ϕ_k depend on the system parameters as described by Eqs. (26). With the form of the master given by Eqs. (30), Eqs. (29) takes the form

$$\begin{aligned}&\ddot{\varepsilon}_1 + \left(\Omega_1^2 + \tfrac{3}{2}\beta A^2\cos(2wt - 2\phi_1)\right)\varepsilon_1\\&\quad + \left(\lambda_0 - \tfrac{3}{2}\mu_1 A^2 w^2\cos(2wt - 2\phi_1)\right)\dot{\varepsilon}_1 + \lambda_1\dot{\varepsilon}_2 = 0,\\&\ddot{\varepsilon}_2 + w_2^2\varepsilon_2 + \gamma\dot{\varepsilon}_2 - \lambda_2\dot{\varepsilon}_1 = 0,\end{aligned} \tag{31}$$

where

$$\lambda_0 = \mu_1\left(\tfrac{3}{2}A^2w^2 - 1\right), \quad \Omega_1^2 = \tfrac{3}{2}\beta A^2 + 1 + K.$$

Setting the following rescalings:

$$\begin{aligned}u(t) &= \varepsilon_1\exp\left\{\frac{\lambda_0}{2}t + \tfrac{3}{8}\mu_1 A^2 w\sin(2wt - 2\phi)\right\},\\v(t) &= \varepsilon_2\exp\left(\frac{\gamma}{2}t\right),\end{aligned} \tag{32}$$

Eq. (31) can be rewritten in the form

$$\begin{aligned}&\ddot{u} + [\delta_{11} + 2\varepsilon_{11}\sin(2wt - 2\phi) + 2\varepsilon_{12}\cos(2wt - 2\phi)\\&\quad + 2\varepsilon_{13}\cos(4wt - 4\phi)]u + \left(\lambda_1\dot{v} + \frac{\gamma\lambda_1}{2}v\right)\exp(\psi(t)) = 0,\end{aligned}$$

$$\ddot{v} + \delta_{21}v + ((\delta_{22} + 2\varepsilon_{21}\cos(2wt - 2\phi_1))u - \lambda_2\dot{u})\exp(-\psi(t)) = 0, \tag{33}$$

where the new parameters $\delta_{ij}, \psi(t)$ and ε_{ij} are given by

$$\begin{aligned}\delta_{11} &= 1 + K + \tfrac{3}{2}\beta A^2 - \frac{3\lambda_0^2}{4} - \tfrac{135}{4}w^4\mu_1^2A^4,\\\delta_{22} &= w_2^2 - \frac{\gamma^2}{4} - \tfrac{3}{4}\lambda_0 w^2\mu A^2,\\\varepsilon_{13} &= \tfrac{81}{64}w^4\mu_1^2A^4, \quad \varepsilon_{12} = \tfrac{3}{4}\beta_1 A^2 - \tfrac{3}{4}w^2\mu_1 A^2,\\\varepsilon_{11} &= -\tfrac{1}{2}w^3\mu_1 A^2, \quad \delta_{21} = w_2^2 + \frac{\gamma^2}{4} - \frac{\gamma}{2},\end{aligned}$$

$$\varepsilon_{21} = \tfrac{3}{8}w^2\mu_1\lambda_2 A^2, \quad \delta_{22} = \frac{\lambda_0\lambda_2}{2}$$
$$\psi(t) = -\tfrac{1}{2}(\gamma - \lambda_0)t - \tfrac{3}{4}\mu_1 w A^2 \sin(2wt - 2\phi).$$

According to the Floquet theory [9,10], the solutions of Eqs. (33) is

$$u(t) = \exp(\theta_1 t)\alpha(t) = \sum_{n=-\infty}^{n=+\infty} \alpha_n \exp(a_n t),$$
$$v(t) = \exp(\theta_2 t)\beta(t) = \sum_{n=-\infty}^{n=+\infty} \beta_n \exp(b_n t), \tag{34}$$

where $a_n = \theta_1 + 2\mathrm{i}nw$, $b_n = \theta_2 + 2\mathrm{i}nw$, and the functions $\alpha(t) = \alpha(t+\pi)$ and $\beta(t) = \beta(t+\pi)$ replace the Fourier series. The quantities θ_1 and θ_2 are two complex numbers, while α_n and β_n are real constants. Inserting Eqs. (34) into Eqs. (33) yields

$$\begin{aligned}
&\sum_{n=-\infty}^{n=+\infty} (\delta_{11} + a_n^2)\alpha_n \exp(a_n t) + ((\varepsilon_{12} + \mathrm{i}\varepsilon_{11})\exp(2\mathrm{i}\phi)) \sum_{n=-\infty}^{n=+\infty} \alpha_n \exp(a_{n-1}t) \\
&\quad + (\varepsilon_{12} - \mathrm{i}\varepsilon_{11})\exp(-2\mathrm{i}\phi) \sum_{n=-\infty}^{n=+\infty} \alpha_n \exp(a_{n+1}t) + \varepsilon_{13}\exp(-4\mathrm{i}\phi)\alpha_n \exp(a_{n+2}t) \\
&\quad + \varepsilon_{13}\exp(4\mathrm{i}\phi)\alpha_n \exp(a_{n-2}t) + \left(\lambda_1 b_n + \frac{\gamma\lambda_1}{2}\right)\exp(\psi(t)) \sum_{n=-\infty}^{n=+\infty} \beta_n \exp(b_n t) = 0, \\
&\sum_{n=-\infty}^{n=+\infty} (\delta_{21} + b_n^2)\beta_n \exp(b_n t) + \exp(-\psi(t)) \sum_{n=-\infty}^{n=+\infty} (\delta_{22} - \lambda_2 a_n)\alpha_n \exp(a_n t) \\
&\quad - \varepsilon_{21}\exp(-\psi(t))\exp(-2\mathrm{i}\phi_1) \sum_{n=-\infty}^{n=+\infty} \alpha_n \exp(a_{n+1}t) \\
&\quad - \varepsilon_{21}\exp(-\psi(t))\exp(2\mathrm{i}\phi_1) \sum_{n=-\infty}^{n=+\infty} \alpha_n \exp(a_{n-1}t) - \lambda_2 \exp(-\psi(t)) = 0.
\end{aligned} \tag{35}$$

Equating each of the coefficients of the exponential functions to zero yields the following infinite set of linear, algebraic, homogeneous equations for the α_m and β_m coefficients:

$$\begin{aligned}
&(\delta_{11} + a_m^2)\alpha_m + ((\varepsilon_{12} + \mathrm{i}\varepsilon_{11})\exp(2\mathrm{i}\phi_1))\alpha_{m+1} \\
&\quad + (\varepsilon_{12} - \mathrm{i}\varepsilon_{11})\exp(-2\mathrm{i}\phi_1)\alpha_{m-1} + \varepsilon_{13}\exp(-4\mathrm{i}\phi_1)\varepsilon_{m-2} \\
&\quad + \varepsilon_{13}\exp(4\mathrm{i}\phi_1)\alpha_{m+2} + \left(\lambda_1 b_m + \frac{\gamma\lambda_1}{2}\right)\exp(\psi(t))\beta_m = 0,
\end{aligned}$$

$$\begin{aligned}
&(\delta_{21} + b_m^2)\beta_m + \exp(-\psi(t))(\delta_{22} - \lambda_2 a_m)\alpha_m \\
&\quad - \varepsilon_{21}\exp(-\psi(t))\exp(-2\mathrm{i}\phi_1)\alpha_{m-1} \\
&\quad - \varepsilon_{21}\exp(-\psi(t))\exp(2\mathrm{i}\phi_1)\alpha_{m+1} = 0.
\end{aligned} \tag{36}$$

For the nontrivial solutions, the determinant of the matrix in Eqs. (36) must vanish. Since the determinant is infinite, we divide the first and second expressions of Eqs. (36) by $(\delta_{11}-4m^2)$ and $(\delta_{21}-4m^2)$, respectively, for convergence considerations. When ε_{ij} are small, approximate solutions can be obtained considering only the central rows and columns of the Hill's determinant. The small Hill determinant for this case has six rows and six columns. Thus, in the first order, Eqs. (36) may have solutions if and only if the associated Hill's determinant is set equal to zero. This condition defines the boundary dividing the parameters space into two domains: the stability and the instability ones. Thus, limiting ourselves to the central rows and columns of the Hill determinant, we find that the boundary separating stability to instability domains is given by

$$\begin{aligned}\Delta(\theta_1,\theta_2) = {} & (\Delta_{12}\Delta_{21}-D_{22}\Delta_{11})\times[(\Delta_{56}\Delta_{63}+\Delta_{66}\Delta_{53})\\ & \times(\Delta_{34}\Delta_{45}-\Delta_{44}\Delta_{35})+(\Delta_{56}\Delta_{65}+\Delta_{66}\Delta_{55})\\ & \times(\Delta_{33}\Delta_{44}-\Delta_{43}\Delta_{34})]-\Delta_{12}\Delta_{56}\Delta_{31}\Delta_{23}\Delta_{44}\Delta_{65}\\ & +\Delta_{22}\Delta_{66}\Delta_{31}\Delta_{53}\Delta_{44}\Delta_{15}-\Delta_{22}\Delta_{66}\Delta_{31}\Delta_{55}\Delta_{13}\Delta_{44}\\ & +\Delta_{22}\Delta_{56}\Delta_{31}\Delta_{44}\times(\Delta_{13}\Delta_{65}-\Delta_{15}\Delta_{63})\\ & -\Delta_{22}\Delta_{66}\Delta_{51}\Delta_{13}\times(\Delta_{34}\Delta_{45}-\Delta_{44}\Delta_{35})\\ & -\Delta_{22}\Delta_{66}\Delta_{51}\Delta_{15}\times(\Delta_{33}\Delta_{44}-\Delta_{43}\Delta_{34})\\ & +\Delta_{12}\Delta_{66}\Delta_{51}\Delta_{23}\times(\Delta_{34}\Delta_{45}-\Delta_{44}\Delta_{35})\\ & +\Delta_{12}\Delta_{66}\Delta_{31}\Delta_{23}\Delta_{44}\Delta_{55}\\ = {} & 0,\end{aligned} \tag{37}$$

where

$$\begin{aligned}&\Delta_{11}=\delta_{11}+(\theta_1-2\mathrm{i}w)^2,\quad \Delta_{12}=\exp(\psi(t))\left(\lambda_1(\theta_2-2\mathrm{i}w)+\frac{\gamma\lambda_2}{2}\right),\\ &\Delta_{13}=(\varepsilon_{12}+\mathrm{i}\varepsilon_{11})\exp(2\mathrm{i}\phi_1),\quad \Delta_{15}=\varepsilon_{13}\exp(4\mathrm{i}\phi),\\ &\Delta_{21}=\exp(-\psi(t))(\delta_{22}-\lambda_2(\theta_1-2\mathrm{i}w)),\quad \Delta_{22}=\delta_{21}+(\theta_2-2\mathrm{i}w)^2,\\ &\Delta_{23}=-\varepsilon_{21}\exp(-\psi(t))\exp(2\mathrm{i}\phi_1),\quad \Delta_{31}=(\varepsilon_{12}-\mathrm{i}\varepsilon_{11})\exp(-2\mathrm{i}\phi_1)\\ &\Delta_{33}=\delta_{11}+\theta_1^2,\quad \Delta_{34}=\exp(\psi(t))\left(\lambda_1\theta_2+\frac{\gamma\lambda_1}{2}\right)\\ &\Delta_{35}=\exp(2\mathrm{i}\phi_1)(\varepsilon_{12}+\mathrm{i}\varepsilon_{11}),\quad \Delta_{43}=\exp(-\psi(t))(\delta_{22}-\lambda_2\theta_1),\\ &\Delta_{44}=\delta_{21}+\theta_2^2,\quad \Delta_{45}=-\varepsilon_{21}\exp(-\psi(t))\exp(2\mathrm{i}\phi_1)\end{aligned}$$

$$\begin{aligned}&\Delta_{51}=\varepsilon_{13}\exp(-4\mathrm{i}\phi_1),\quad \Delta_{53}=(\varepsilon_{12}-\mathrm{i}\varepsilon_{11})\exp(-2\mathrm{i}\phi_1),\\ &\Delta_{55}=\delta_{11}+(\theta_1+2\mathrm{i}w)^2,\quad \Delta_{56}=\exp(\psi(t))(\lambda_1(\theta_2+2\mathrm{i}w)+\gamma\lambda_1/2)\\ &\Delta_{63}=\varepsilon_{21}\exp(-\psi(t))\exp(-2\mathrm{i}\phi_1),\quad \Delta_{65}=\exp(-\psi(t))(\delta_{22}-\lambda_2(\theta_1+2\mathrm{i}w))\\ &\Delta_{66}=\delta_{22}+(\theta_2+2\mathrm{i}w)^2.\end{aligned}$$

Since, we have

$$\varepsilon_1(t) = \exp\left\{\left(\theta_1 - \frac{\lambda_0}{2}\right)t - \frac{3\mu_1 w A^2}{8}\sin(2wt - 2\phi)\right\}\alpha(t),$$
$$\varepsilon_2(t) = \exp\left(\left(\theta_2 - \frac{\gamma}{2}\right)t\right)\beta(t), \tag{38}$$

the Floquet theory states that the transition from stability to instability domains (or the reverse) occurs only in the two conditions:

- π-periodic transitions (periodic motion with period π) at $\theta_1 = \theta_1^{1c} = \lambda_0/2$ and $\theta_2 = \theta_2^{1c} = \gamma/2$.
- 2π-periodic transitions (periodic motion with period 2π) at $\theta_1 = \theta_1^{2c} = i + \lambda_0/2$ and $\theta_2 = \theta_2^{2c} = i + \gamma/2$.

Thus replacing θ_i by θ_i^{ic} $(i = 1, 2)$ in Eq. (37), we obtain an equation which helps to determine the range of K in which the synchronization process is stable. The amplitude $A = 0.85$ and the frequency $w = 0.64$ used are resorted from the numerical simulation of Eq. (27) with the parameters of Fig. 7 and $\gamma = 0.1$. From Eq. (37), the stability is achieved for $K \in]-1.9; -0.304[\cup]0; +\infty[$ as it appears in Fig. 9. These results obtained are verified by a direct numerical simulation of equations (27) with the sixth-order formulas of the Butcher family of the Runge–Kutta algorithm [15]. The master and the slave are initially launched with the following appropriate initial conditions $(x(0), \dot{x}(0), y(0), \dot{y}(0)) = (5.0, 5.0, 0.0, 0.0)$ and $(u(0), \dot{u}(0), v(0), \dot{v}(0)) = (4.0, 4.0, 0.0, 0.0)$, respectively. The synchronization process is launched at $T_0 = 200$ and K is varied until the synchronization is achieved (here, synchronization is achieved when the deviation ε_1 obeys the following synchronization condition $\varepsilon_1 = |x - u| < h,\ \forall t > T_0$ with $h = 10^{-10}$). With the numerical procedure, we find that the stability of the synchronization process requires that $K \in]-1.6; -0.57[\cup]0.0008; +\infty[$. The agreement between the analytical and numerical results is quite acceptable. Indeed, it is expected that the gap between the analytical and numerical results could be reduced by including the nonlinearity effects through the variational equations. In fact, for the domain $K \in]-1.9; -1.6] \cup [-0.57; -0.304]$ (difference between the analytical and numerical domains), the numerical procedure shows that the slave is stable but the synchronization is not achieved, since $\varepsilon_i(t)$ does not vanish but remains a bounded oscillatory function (see Figs. 10 and 11).

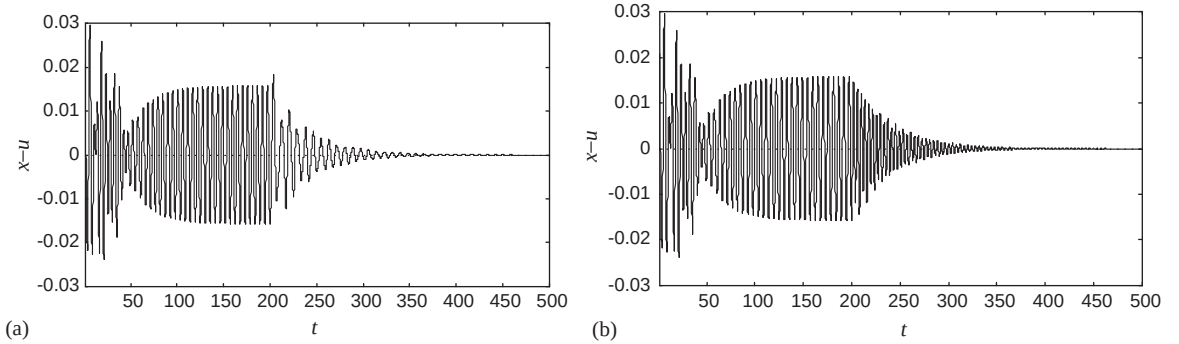

Fig. 9. Time history of the deviation $\varepsilon_1(t)$ with the parameters defined in Fig. 7, (a) $K = -1$ and (b) $K = 1$.

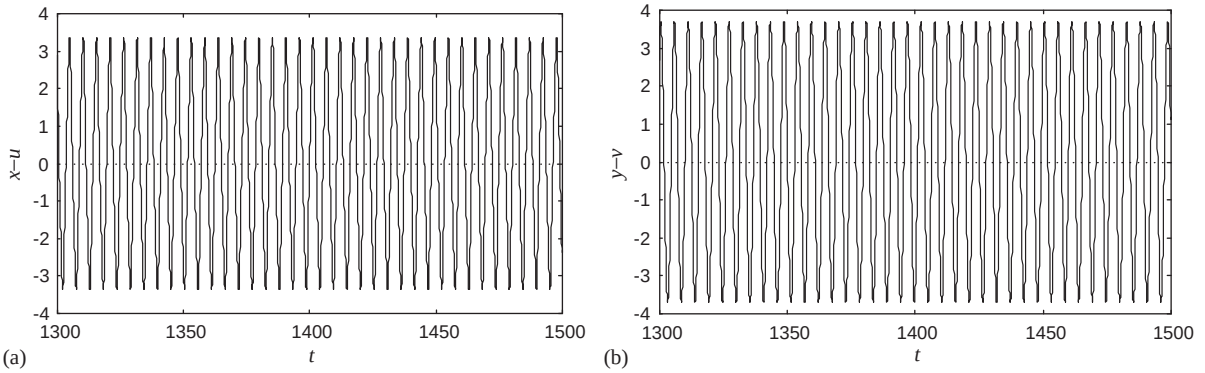

Fig. 10. Time history of the deviation $\varepsilon_1(t)$ (a) and $\varepsilon_2(t)$ (b) with the parameters defined in Fig. 7 and $K = -1.8$.

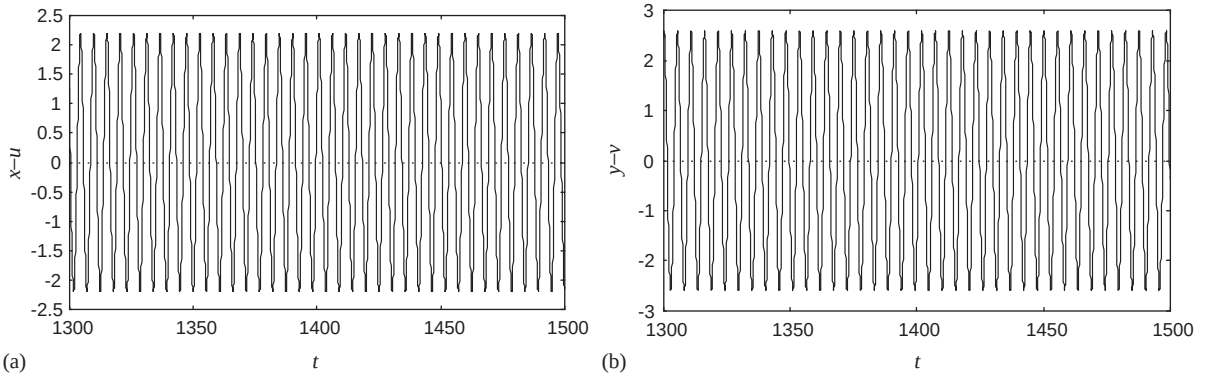

Fig. 11. Time history of the deviation $\varepsilon_1(t)$ (a) and $\varepsilon_2(t)$ (b) with the parameters defined in Fig. 7 and $K = -0.3$.

The synchronization time T_s is plotted versus K and the results are reported in Fig. 12 with the following synchronization precision $h = 10^{-10}$. There appears from this figure a singularity around the value of $K = 0.3$, this singularity can be understood by the presence of the possible parametric resonances in the variational equations, which manifests itself here by the high value of the synchronization time [22].

4. Conclusion

This paper has dealt with the dynamics and synchronization of self-sustained electromechanical devices consisting of an electrical Rayleigh–Duffing oscillator coupled magnetically to a mechanical linear oscillator. The synchronization process of two self-sustained electrical models described by the Rayleigh–Duffing oscillator has first been considered. The analytical investigation has been based on the properties of the Hill equation which describes the deviation between the slave and the master oscillators. The synchronization boundaries have been obtained, as well as the expressions of the synchronization time. Secondly, the dynamics and

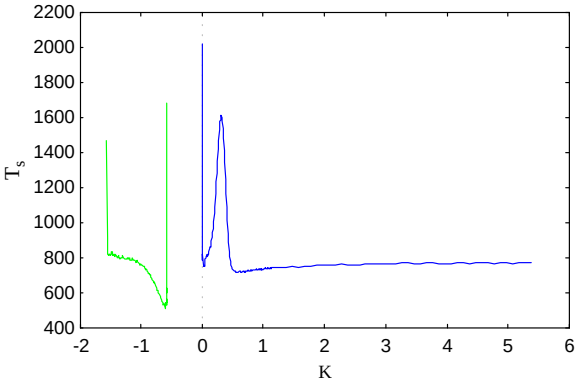

Fig. 12. Synchronization time T_s versus K with the parameters of Fig. 7 and $\gamma = 0.1$, $h = 10^{-10}$.

synchronization of coupled self-sustained electromechanical devices have also been considered. The amplitudes of the oscillatory states have been derived using the averaging method. The stability boundaries of the synchronization process have been derived using the Floquet theory.

An extension of the study to a large number of electromechanical devices is an interesting task, which can be tackled using a series of cascading control (the master controls the first slave, which in its turn controls the second slave, etc.) or a mutually coupling scheme (a sort of network of electromechanical devices).

References

[1] L.M. Pecora, T.L. Caroll, Synchronization in chaotic systems, *Physical Review Letters* 64 (1990) 821–824.
[2] T. Kapitaniak, Synchronization of chaos using continuous control, *Physical Review E* 50 (1994) 1642–1644.
[3] K. Pyragas, Continuous control of chaos by self-controlling feedback, *Physics Letters A* 170 (1992) 421–428.
[4] A.V. Oppenheim, G.W. Wornell, S.H. Isabelle, K. Cuomo, Signal processing in the context of chaotic signals, *Proceedings of the International Conference on Acoustic, Speech and Signal Processing*, IEEE, New York, vol. I4, 1992, pp. 117–120.
[5] L.J. Kocarev, K.S. Halle, K. Eckert, U. Parlitz, L.O. Chua, Experimental demonstration of secure communications via chaotic synchronization, *International Journal of Bifurcation and Chaos* 2 (1992) 709–713.
[6] G. Perez, H.A. Cerdeira, Extracting messages masked by chaos, *Physical Review Letters* 74 (1995) 1970–1973.
[7] A.T. Winfree, *The Geometry of Biological Time*, Springer, New York, 1980.
[8] Y. Kuramoto, *Chemical Oscillations, Waves and Turbulence*, Springer, Berlin, 1980.
[9] C. Hayashi, *Nonlinear Oscillations in Physical Systems*, Mc-Graw-Hill, New York, 1964.
[10] A.H. Nayfeh, D.T. Mook, *Nonlinear Oscillations*, Wiley-Interscience, New York, 1979.
[11] W. Szemplińska-Stupnicka, J. Rudowski, Neimark bifurcation, almost-periodicity and chaos in the forced Van der Pol–Duffing system in the neighbourhood of the principal resonance, *Physics Letters A* 192 (1994) 201–206.
[12] A. Venkatesan, M. Lakshamanan, Bifurcation and chaos in the double-well Duffing–Van der Pol oscillator: numerical and analytical studies, *Physical Review E* 56 (1997) 6321–6330.
[13] A. Oksasoglu, D. Vavriv, Interaction of low- and high-frequency oscillations in a nonlinear RLC circuit, *IEEE Transactions on Circular Systems—I* 41 (1994) 669–672.
[14] M.J. Hasler, Electrical circuits with chaotic behavior, *Proceedings of the IEEE* 75 (1987) 1009–1021.
[15] H.K. Leung, Critical slowing down in synchronizing nonlinear oscillators, *Physical Review E* 58 (1998) 5704–5709.

[16] P. Woafo, R.A. Kraenkel, Synchronization: stability and duration time, *Physical Review E* 65 (2002) 036225.
[17] L. Lapidus, J.H. Seinfeld, *Numerical Solution of Ordinary Differential Equations*, Academic Press, New York, London, 1971.
[18] H.F. Olson, *Acoustical Engineering*, Van Nostrand, Princeton, NJ, 1967.
[19] B.G. Korenev, L.M. Reznikov, *Dynamics Vibration Absorbers*, Wiley, New York, 1989.
[20] K.R. Asfar, Quenching of self-excited vibrations, *Journal of Vibration and Acoustics, Stress and Reliability in Design* 111 (1989) 130–133.
[21] J.C. Chedjou, P. Woafo, S. Domngang, Shilnikov chaos and dynamics of a self-sustained electromechanical transducer, *Journal of Vibrations and Acoustics* 123 (2001) 170–174.
[22] Y. Chembo Kouomou, P. Woafo, Stability and optimization of chaos synchronization through feedback coupling with delay, *Physics Letters A* 298 (2002) 18–28.